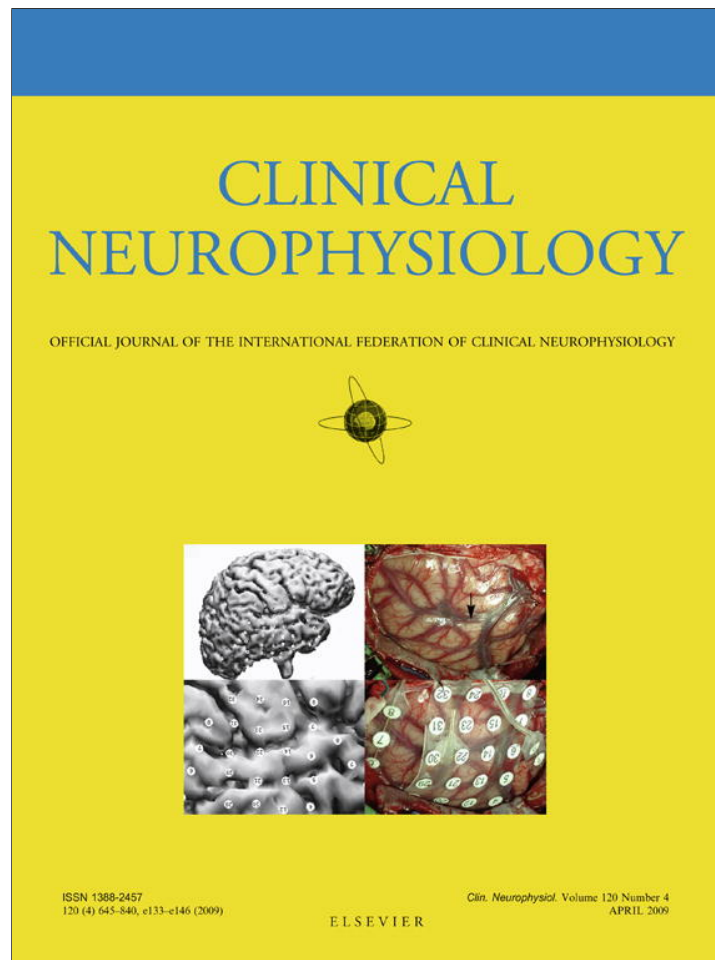


Provided for non-commercial research and education use.
Not for reproduction, distribution or commercial use.

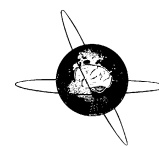


This article appeared in a journal published by Elsevier. The attached copy is furnished to the author for internal non-commercial research and education use, including for instruction at the authors institution and sharing with colleagues.

Other uses, including reproduction and distribution, or selling or licensing copies, or posting to personal, institutional or third party websites are prohibited.

In most cases authors are permitted to post their version of the article (e.g. in Word or Tex form) to their personal website or institutional repository. Authors requiring further information regarding Elsevier's archiving and manuscript policies are encouraged to visit:

<http://www.elsevier.com/copyright>



EEG synchrony during a perceptual-cognitive task: Widespread phase synchrony at all frequencies

Susan Pockett^{a,*}, Gary E.J. Bold^a, Walter J. Freeman^b

^a Department of Physics, University of Auckland, Private Bag 92019, Auckland, New Zealand

^b Department of Cell and Molecular Biology, University of California, Berkeley, USA

ARTICLE INFO

Article history:

Accepted 13 December 2008

Available online 27 February 2009

Keywords:

EEG
Phase synchrony
Global synchrony
Broad band phase
Theta
Alpha
Beta
Gamma
High gamma
Epsilon

ABSTRACT

Objectives: (1) To examine the validity of comparing the phase of broad-band signals. (2) To measure phase synchrony over the whole head, at a variety of frequencies.

Methods: The concept of broad band phase is investigated (a) by visual comparison of the time series of two channels of filtered data with the time series of the spatial analytic phase difference (SAPD) between the two channels and (b) using artificial sinusoids. Phase synchrony is then measured in 64-channel EEG recorded while human subjects performed a perceptual-cognitive task, by calculation of analytic phase differences between each channel and a frontal synchrony reference channel. The number of channels in synchrony with the reference channel at a series of frequency passbands is compared for data acquired using a common recording reference, the same data re-referenced to an average reference and artificial noise.

Results: Analytic phase is shown to represent the resultant of the phasor angles of all the narrow band signals incorporated in a composite waveform. Episodic global phase synchrony is identified in background EEG, in all passbands from theta to epsilon. Many of the episodes of widespread synchrony occur in both common-referenced and average-referenced data, but some common-reference episodes are not seen in average-referenced data. In both forms of data, synchrony is about equally widespread in all subjects at lower passbands, but more widespread in some subjects than others at higher passbands.

Conclusions: (1) It is valid to measure the analytic phase of broad band EEG signals. (2) Non-local phase synchrony is intermittently present in all frequency bands from theta to epsilon, not only during and after external stimuli, but also in background EEG. (3) In some subjects synchrony is more widespread in gamma and epsilon bands than in beta, alpha or delta bands, but in others the reverse is true. (4) Some of the episodes of synchrony seen in common referenced data may be artifacts of a sudden decrease in power at the recording electrodes in comparison with the common reference electrode. However, most of the episodes of synchrony in common-referenced data cannot be explained in this fashion. (5) Episodes of widespread synchrony are not established instantaneously. During the establishment of most episodes of '40 Hz' synchrony, the number of channels in synchrony peaks after about 100 ms.

Significance: If long-range phase synchrony really is a hallmark of consciousness, it should be present most of the time the subject is conscious. Our results confirm this prediction, and suggest that consciousness may involve not only gamma frequencies, but the whole range from theta to epsilon. The mechanism of synchrony establishment at the scalp as shown by the present method is relatively slow and thus more likely to involve chemical synapses than gap junctions, electric fields or quantum non-locality.

© 2009 International Federation of Clinical Neurophysiology. Published by Elsevier Ireland Ltd. All rights reserved.

1. Introduction

Synchronous activity in the brain has now been studied in connection with the neural correlates of consciousness for more than a

decade. Most authors have concentrated on a single frequency band, usually gamma. For example, early work using multiunit recording in cat visual cortex (Engel et al., 1991a) demonstrated the existence of interhemispheric synchronization in the gamma range. This suggested the influential hypothesis that synchrony of firing between widely separated areas of cortex may be the answer to the binding problem, producing "dynamic representation

* Corresponding author. Tel.: +64 9 373 7599; fax: +64 9 373 7445.

E-mail address: s.pockett@auckland.ac.nz (S. Pockett).

of objects by assemblies of synchronously oscillating cells" (Engel et al., 1991b). Further single cell animal data (Engel et al., 2001) were taken to support this idea, although evidence (Lamme and Spekreijse, 1998) and arguments (Shadlen and Movshen, 1999) against it had already been advanced.

In humans, where invasive single cell recording poses formidable ethical and logistic difficulties, the situation is even less straightforward. EEG data are easy to collect, but methods of measuring phase synchrony in them are fraught with pitfalls. For example, Fein et al. (1988) have rejected the idea that synchrony can validly be measured in data recorded using a common recording reference. They point out that it is theoretically possible for low power under both of two recording electrodes to exaggerate the common contribution of the reference electrode, so that any coherence or synchrony measures are essentially comparing the reference with itself. Active recording references can also be problematic in other ways. For example, Rodriguez et al. (1999), measuring synchrony between scalp EEG electrodes, famously reported that when human subjects viewed ambiguous visual stimuli that could be perceived either as a face or as a meaningless pattern of light and dark, "only face perception induces a long-distance pattern of synchronization, corresponding to the moment of perception itself and to the ensuing motor response". However, a later attempt to replicate this result found significant background synchrony for both face and non-face percepts and reported that phase synchrony differences between face perception and non-face perception could be reproduced only if data were recorded against a nose reference, which was shown to be contaminated by microsaccades (Trujillo et al., 2005).

Of course, if long-range synchrony really is a general correlate of consciousness, it must logically be present not just in the brief period following an experimental stimulus, but for more or less the whole time a subject is awake. On this reasoning, synchrony induced by any particular external stimulus *should* be superimposed on significant background synchrony. It is thus fortunate for the hypothesis that synchrony is essential for consciousness that significant background synchrony has also been reported by Freeman and colleagues, both in ECoG measurements from a grid of electrodes implanted on the surface of rabbit sensory cortex (Freeman and Rogers, 2002; Freeman, 2004a,b) and in EEG measurements from human scalp (Freeman et al., 2003a,b).

In the above studies, phase synchrony was measured using various methods of comparing analytic phase, a quantity derived from Hilbert transformed data. These methods revealed spatial patterns of synchronized beta-gamma oscillations emerging after sudden jumps in cortical activity which the authors named 'state transitions'. Each state transition began with an abrupt phase re-setting to a new value on every channel, followed by re-synchronization, spatial pattern stabilization and increase in pattern amplitude. However, one perceived difficulty with these studies has been that they involve comparison between different electrodes of the phase of a broad band signal (12–30 Hz in humans and 20–80 Hz in rabbits). To a traditional physicist, the concept of phase has meaning only in the context of narrow band signals (Pikovsky et al., 2001; Bhattacharya and Petsche, 2005). Hence some concern has been expressed about the validity of results generated by comparison of the phase of two or more broad band signals.

The present investigation aimed: (1) to introduce a new method of calculating inter-electrode synchrony, which has a time resolution limited only by the sampling rate of the data; (2) to unpack the concept of broad band phase and investigate the validity of comparing the phase of two broad band signals using the new metric; (3) to extend earlier work by asking whether or not background synchrony occurs during a perceptual/cognitive task in a series of both narrow and broad frequency passbands; (4) to compare synchrony calculated in data recorded using a common reference with

the same data re-referenced to an average reference; and (5) to ask how long it takes for any particular episode of synchrony to become established.

2. Methods

Data from six male subjects were analysed. The subjects were aged 23–44. All but one (subject JL) were right handed. Data were collected in the Psychology Dept of the University of California Berkeley and the study was approved by the UC Berkeley Institutional Review Board. All subjects gave informed consent.

Each subject participated in a single 60–90 min session, during which 64-channel EEG data were recorded while a series of paired visual and auditory stimuli were presented. The details of the task are essentially irrelevant to the present analysis, but are given here for completeness. The visual stimuli consisted of a 125 ms flash during which a computer screen positioned in front of the participant's chair turned either entirely red or entirely blue. The auditory stimulus was either a comfortably loud or a much softer 100 ms burst of white noise from two computer speakers positioned to either side of the screen. Three stimulus pairs were delivered at random: Red-Loud, Blue-Soft or Blue-Loud. The subject's task was to learn by trial and error which of three computer keys to press in response to each of the stimulus pairs. The keyboard was placed on the subject's lap and their hand comfortably supported in such a position that no gross arm movements were necessary in order to press one of the three keys. Keys were pressed with the right hand. As soon as a response key was pressed, feedback ("Correct! Well Done" or "Incorrect. Better luck next time") was presented in white text on a black screen. After 1 s this text was replaced by a white fixation cross in the middle of a black screen, which lasted until the next stimulus pair was delivered. Subjects were instructed to maintain their gaze on the location of the fixation cross throughout the experiment and to avoid blinking until the period between key press and the next stimulus. Any trials where a blink (as detected by later visual inspection of the EEG time series at pre-frontal channels) did occur between stimulus and response were excluded from further analyses. For the first 180 stimulus presentations, positive or negative feedback was delivered at random, so that it was impossible to score 100% correct answers. For the next 200 presentations, "Correct" feedback was delivered if key 1 was pressed for Red-Loud stimuli, key 2 for Blue-Soft and key 3 for Blue-Loud. Most subjects scored 95–100% correct answers after the first 3–10 trials in this second block.

EEG was recorded using BioSemi™ amplifiers with a 64-electrode cap. Sintered Ag/AgCl electrodes were interfaced with the scalp using Signigel (Parker). Approximate positions of the electrodes are shown in Fig. 1. The BioSemi system records data referenced to a point between their CMS and DRL electrodes (not shown), to which the closest approximation is electrode POz (Channel 30). Data were digitised at a sampling rate of 512 Hz, with an analog pass band of DC to 134 Hz. Continuous records were taken, with the times of various sorts of stimuli and responses marked in a 65th recording channel.

2.1. Signal processing

Stored data were converted offline to Matlab™ format using the BioSig conversion facility available in EEGLAB (Delorme and Makeig, 2004). Specified data epochs surrounding individual key presses were extracted from the continuous record, sometimes rereferenced to an average reference, then locally detrended, band-pass filtered, and further processed using purpose-written Matlab routines. Time measurements were made using the Matlab 'data-tip' facility. *Bandpass filtering* was performed by applying a FIR filter to data that had been lengthened by appending an inverted copy

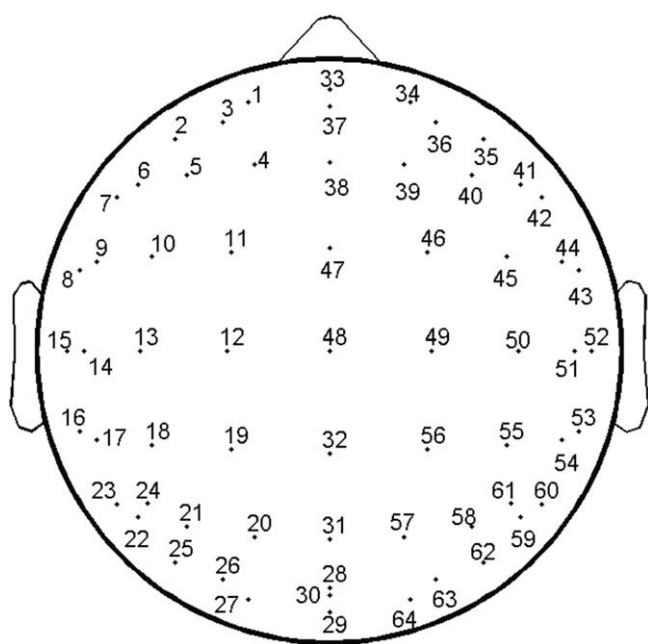


Fig. 1. Channel locations.

of the original data to each end of the data segment. After filtering, the original length of the time series was reinstated by removal of the copies. *Power density spectra* were produced by applying the Matlab command 'pwelch' to the spatial ensemble average (a dataset constructed by averaging at each point in the time series the data from all 64 channels). *Scale-free $1/f^{1.5}$ noise* was generated using the Matlab code available at <http://www.mathworks.com/matlabcentral/fileexchange/loadFile.do?objectId=5091&objectType=file>. A beta value of -1.5 was chosen, because this represented the slope of the log–log plot of subject FS's power density spectrum. To obtain spatially uncorrelated or independent noise, the method for generating an individual time series was used 64 times to generate 64 channels of noise.

2.2. Analytic phase and analytic power

The *analytic signal* or analytic representation of a real-valued signal $x(t)$ is defined by $x_a(t) = x(t) + j(\hat{x}(t))$, where j is the imaginary operator and $\hat{x}(t)$ is the Hilbert transform (Bracewell, 1965) of $x(t)$, which is generated by convolving $x(t)$ with $\frac{1}{\pi t}$. The Matlab command 'hilbert' generates analytic signals. *Analytic power* is the square of the real part of the analytic signal plus the square of the imaginary part of the analytic signal: $[(\text{real}(x_a(t)))^2 + (\text{imag}(x_a(t)))^2]$. The time series of *analytic phase* is a vector of angles defined by $\theta = \arctan \frac{\text{imag}(x_a(t))}{\text{real}(x_a(t))}$ and is conveniently calculated using the Matlab command 'angle'. To facilitate intuitive understanding of these measures, Fig. 2 illustrates the relationship of analytic phase and analytic power to the raw signal. Fig. 2A shows a segment of raw EEG. Fig. 2B shows its bandpass filtered version. Fig. 2C shows the real (black) and imaginary (gray) parts of the analytic signal. It can be seen that the imaginary part of the analytic signal is phase-shifted by $\frac{\pi}{2}$ radians or 90° from the real part. Fig. 2D shows how analytic phase ramps between $-\pi$ and π radians with each cycle of the original signal. Fig. 2E shows analytic phase unwrapped using the Matlab command 'unwrap'. The relationship between analytic power and the square of the original signal can be seen in Fig. 2F – basically, analytic power scribes out the envelope of the rectified (i.e. squared) filtered signal.

The physical meaning of broad band analytic phase is investigated and explained in Appendix A and discussed in Section 4.

2.3. Phase synchrony index

A new phase synchrony index, the spatial analytic phase difference (SAPD) was derived by calculating and unwrapping analytic phase, and then for each point in the time series taking the absolute value of the difference between the instantaneous phase of data from the chosen synchrony reference channel and the instantaneous phase of data from each channel to be compared with the reference. The synchrony reference channel was channel 1 (FP₁) for channels 1–33 (i.e. all channels over the left hemisphere) and channel 34 (FP₂) for channels 34–64 (i.e. all the channels over the right hemisphere). These phase differences were then projected back into the interval $[0, 2\pi]$ as the remainder after division by 2π , using the Matlab command 'mod'. Since the maximum possible phase difference is π , values in the interval $[\pi, 2\pi]$ were projected back into the interval $[0, \pi]$ by subtracting them from 2π . The resulting values, one for each point in the time series, were called SAPD values. An SAPD value of 0 radians indicates perfect in-phase synchrony between the two channels of interest, at that time point. An SAPD value of π radians indicates perfect 180° out-of-phase synchrony. SAPD values between 0 and π indicate progressively less synchrony as the value approaches the mid point between 0 and π .

To calculate the number of channels in synchrony with the frontal reference channels at each point in the time series, SAPD values <0.2 radians were taken as indicating in-phase synchrony. All SAPD values less than 0.2 radians were replaced by the number 1 and all other SAPD values by 0. The number of 1s in each column of the resulting matrix was then summed, to give a maximum possible number of channels in synchrony of 64.

In the *Supplementary Movies*, SAPD values at each time point were plotted as a function of the recording channel's position on the head, as sets of 64 false color values. Dark red represents a spatial analytic phase difference of 0, i.e. perfect in-phase synchrony. Dark blue represents a spatial analytic phase difference of π radians, i.e. perfect out-of-phase synchrony. The 64 intermediate colors represent phase differences that increase by $\pi/64$ radians for each color gradation. The movies are made using either data acquired with a common recording reference, or independent noise.

3. Results

3.1. The SAPD metric and the concept of broad band phase

Fig. 3 compares the time series of two channels of filtered data (the red¹ channel offset by 10 μV for ease of comparison) with the time series of the SAPD (spatial analytic phase difference) between them. It can be seen that during time periods when the two channels appear to be perfectly in phase (i.e. waxing and waning in identical fashion) the SAPD is low. In time periods when the two channels are not in synchrony, the SAPD is high. The pass band of the filter is 12–30 Hz, which makes this a relatively broad band signal.

3.2. Phase synchrony in data filtered into different passbands

For each point in the time series, data were either re-referenced to the average value of all channels at that time point (i.e. average-referenced), or left as the originally recorded common-referenced

¹ For interpretation of the references to color in Fig. 3, the reader is referred to the web version of this paper.

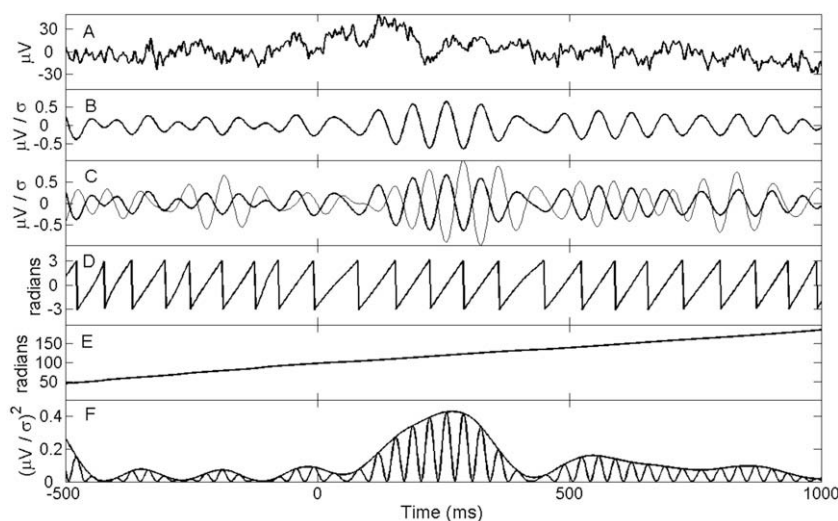


Fig. 2. Relationship of analytic phase and power to original signal. (A) Raw signal (FS Epoch 28 Channel 1). (B) Detrended and bandpass filtered signal (passband 12–17 Hz). (C) Real (black) and imaginary (gray) parts of analytic signal. (D) Analytic phase. (E) Unwrapped analytic phase. (F) Analytic power and rectified (squared) version of B.

data. Both kinds of data and also independent noise were then filtered into passbands representing the traditional theta, alpha, beta and gamma bands, with the addition of the very high frequency band epsilon. For each pass band, phase synchrony between each channel and channel FP1 (left hemisphere) or FP2 (right hemisphere) was measured using the SAPD metric. Taking SAPD values <0.2 radians as representing in-phase synchrony, the number of channels in synchrony with the prefrontal channels was then calculated for each point in the respective time series. The graphs presented in Figs. 3–10 show results for one epoch in one subject, but are representative of similar results found by analysing other epochs in this subject and the other five subjects.

Fig. 4 shows a time series of the number of channels in synchrony in Epoch 28 of subject FS's data, for noise, average and common referenced data filtered into the traditional gamma pass band, 37–43 Hz. The standard deviation of the number of channels in synchrony for each of the two kinds of data and noise is shown as a horizontal dashed line in the same color as the relevant dataset.

Three findings are evident from this plot.

- (1) In both common- and average-referenced data, but not in noise, intermittent peaks of relatively high synchrony project above a baseline of fluctuating but low synchrony. In

the data, the distribution of number of channels in synchrony is highly skewed, with most time points having values in the baseline and relatively few time periods showing a large number of synchronous channels. Analysis with the non-parametric Wilcoxon rank sum test shows that the median number of channels in synchrony over a 3 s time period in either average or common referenced data is highly significantly different from that in noise ($p < 0.0001$).

- (2) The peaks of widespread synchrony are lower (fewer channels in synchrony) for average-referenced than common-referenced data, but they almost all occur at the same times. For most of the peaks in the common-referenced data, a concomitant peak is evident in the average-referenced data.
- (3) Episodes of widespread synchrony are not established instantaneously. The time taken for most episodes to rise from baseline to peak number of channels in synchrony is of the order of 100 ms. For the peaks where rise-times are indicated as 90 ms and 101 ms, the points between which time to peak was measured are indicated with black arrowheads.

Fig. 5 repeats Fig. 4 for a wider gamma passband, 30–58 Hz. Now the episodes of synchrony in the common-referenced data are shorter and more numerous, and fewer of them are associated

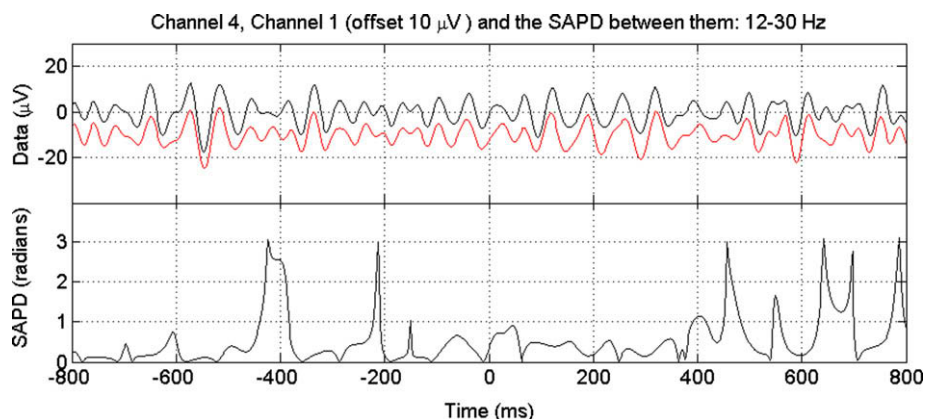


Fig. 3. Time series for two channels of data and the SAPD between them.

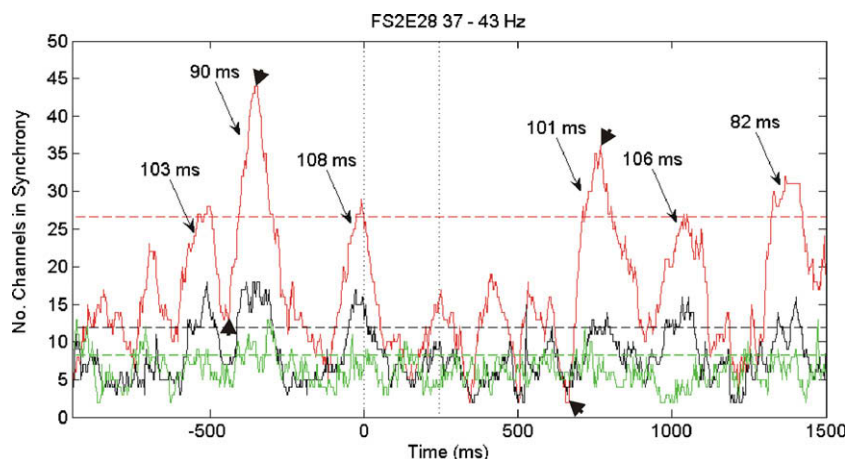


Fig. 4. Time series of number of channels in synchrony with FP1 (channels 1–33) or FP2 (channels 34–64) for signals filtered at 37–43 Hz. Red: common-referenced data. Black; average-referenced data. Green: noise. Vertical dotted lines indicate onset and offset of stimulus. Horizontal dashed lines show (mean + one standard deviation) of the number of channels in synchrony for common-referenced data (red), average-referenced data (black) and noise (green). Numbers above arrows indicate milliseconds from base to peak. For the peaks where these times are indicated as 90 ms and 101 ms, respectively, the positions between which the times were measured are indicated with black arrowheads. (For interpretation of the references to color in this figure legend, the reader is referred to the web version of this paper.)

with a concomitant peak in the average-referenced data – but some still are. Fig. 6 shows a similar picture for the high gamma or epsilon (Freeman, 2007) passband, 80–130 Hz. Again, for both passbands the median number of channels in synchrony in either average- or common-referenced data is significantly different from that in noise ($p < 0.0001$).

Fig. 7 deals with the beta passband 12–30 Hz. Note the expanded time axis. Now the episodes of synchrony in common-referenced data are less widespread than in the gamma passbands, although the median number of channels in synchrony is again different from noise at $p < 0.0001$ for both common- and average-referenced data. As with the “40 Hz” passband, almost all common-referenced episodes occur at the same time as similar average-referenced episodes. In this figure only the common-reference peaks at around 500 ms and –700 ms are not associated with concomitant average-reference peaks. The lower end of the beta passband (12–17 Hz) is shown in Fig. 8. Now more of the common-reference synchrony peaks are not associated with average-reference peaks. This pattern is repeated for the alpha (8–12 Hz) and theta passbands (4–8 Hz), which are illustrated by Figs. 9 and 10, respectively. At all of 12–17 Hz, 8–12 Hz and 4–8 Hz, the median number of channels in synchrony in both common- and average-referenced data is different from noise at $p < 0.0001$ (Wilcoxon rank sum test).

3.3. Reproducibility

Plots like those shown in Figs. 4–10 were made for four randomly selected blink-free epochs from each of the six subjects. Supplementary Figs. S1–S12 show such results for the low beta (12–17 Hz) and traditional gamma (37–43 Hz) passbands. It can be seen that subjects vary slightly – in particular, some subjects show more widespread gamma synchrony than others – but roughly the same pattern of episodic synchrony occurs in all subjects. These and other data indicate that in all subjects, the rise time of individual episodes of widespread synchrony is of the order of 100 ms in data filtered into 5–6 Hz wide passbands of all centre frequencies. In general terms, the rise time of individual episodes of synchrony was observed to decrease as the filter passband became wider (compare Fig. 6 with the bottom right panel of Fig. 13). The duration of individual frames of analytic power was also observed to decrease as the filter passband became wider.

Visual inspection of Supplementary Figs. S1–S12 shows no obvious temporal pattern of occurrence of either beta or gamma synchrony in relation to stimulus onset. Episodes of synchrony do not appear to be stimulus-locked in any reproducible way. No statistical analysis of this question was done, so it remains conceivable that future analyses might reveal some degree of cryptic stimulus-locking, but none is obvious to the naked eye.

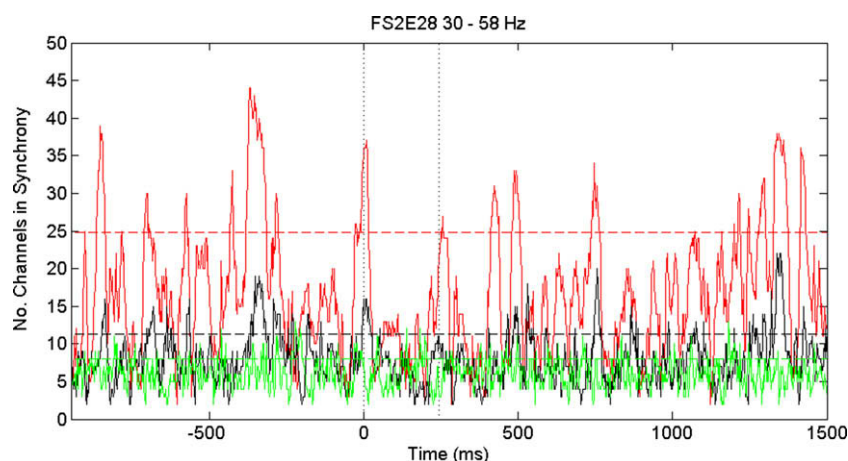


Fig. 5. Time series as for Fig. 4: 30–58 Hz.

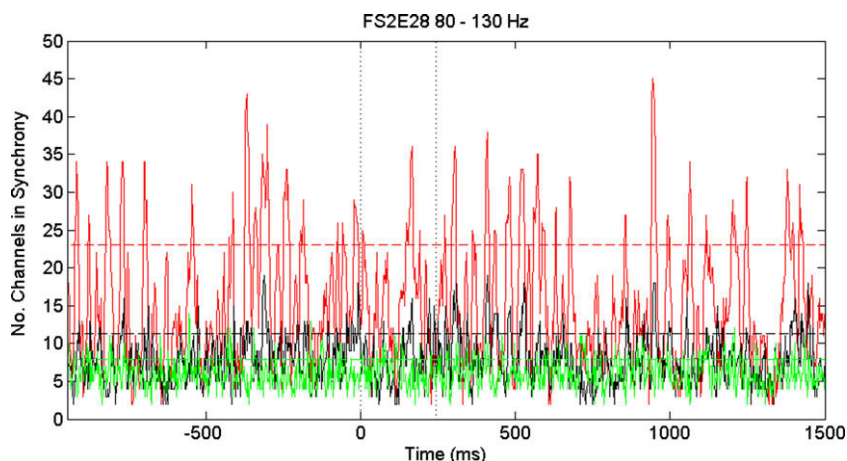


Fig. 6. Time series as for Fig. 4: 80–130 Hz.

3.4. Spatial patterns of synchrony

The evolving spatial patterns of channels synchronous with the two prefrontal reference channels in all passbands are shown in the [Supplementary Movies](#). In these presentations, the bar to the left of the head turns increasingly yellow during the period before both stimulus and response, then turns red while the auditory-visual stimulus is present and briefly blue when the subject's response occurs. More importantly, the changing colors within the head indicate the degree of synchrony between each electrode on the head and the electrode at FP1 (for electrodes over the left half of the head) or FP2 (for electrodes over the right). Dark red indicates zero phase difference (i.e. perfect synchrony) and dark blue indicates 180° phase difference (i.e. perfect antisynchrony). It can be seen that in data at all frequency passbands, the red color indicating in-phase synchrony flows around the head, intermittently becoming truly global, but interspersed with flashes of green (absence of synchrony) and blue (out-of-phase synchrony). Episodes of global synchrony are never seen in the movies of independent artificial noise.

3.5. Effects of muscle noise

Fig 11 shows the effect of muscle noise at the synchrony reference channel. Fig. 12 shows the effect of muscle noise at a common recording reference channel. Fig. 13 shows the effect of a blink.

4. Discussion

The results presented here both confirm and extend the earlier findings of Freeman et al. (2003a,b). In confirmation of the earlier studies, intermittent long-range synchrony between the oscillations recorded at different channels was clearly seen in EEG data filtered into the relatively broad pass band 12–30 Hz.

In extension of the earlier results:

- (1) Brief episodes of fully global synchrony, involving the entire head and not just the 189 mm distance which is the longest previously examined, were observed in all subjects, in all pass bands studied from theta to epsilon, and in both broad and narrow band filtered data.
- (2) Episodes of widespread synchrony were not confined to any particular time period with relation to stimulus onset, but occurred throughout the dataset.
- (3) Episodes of widespread synchrony generally involved more channels in gamma and epsilon bands than in beta, alpha or delta bands.
- (4) No similar episodes of widespread synchrony were observed in spatially uncorrelated $1/f^\alpha$ noise.
- (5) Episodes of widespread synchrony were not established instantaneously on the abrupt phase jumps described in earlier work, but built up over approximately 100 ms.

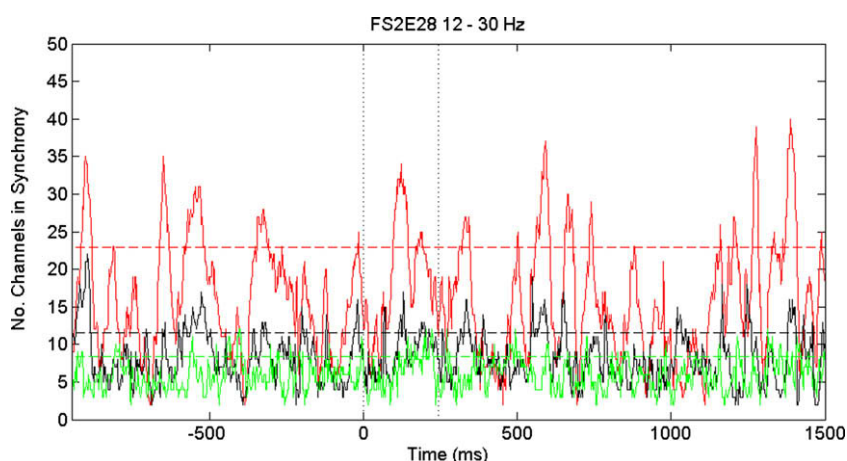


Fig. 7. Time series as for Fig. 4: 12–30 Hz.

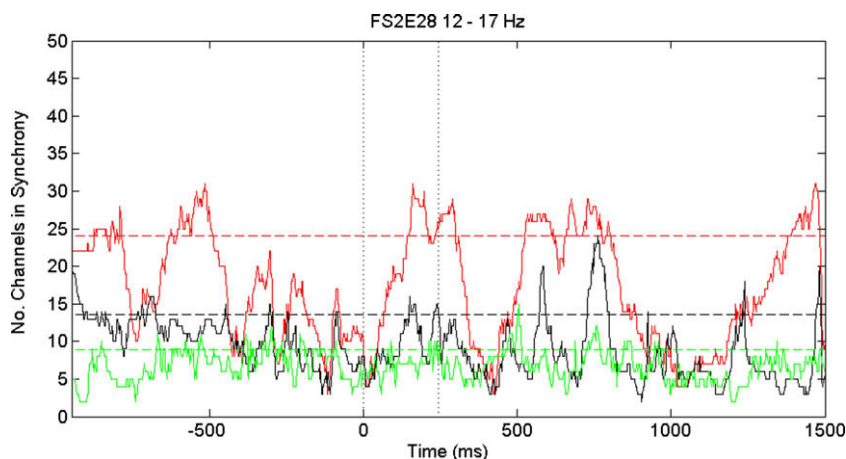


Fig. 8. Time series as for Fig. 4: 12–17 Hz.

4.1. What does “phase” mean in the context of a broad band signal?

One of the initial aims of the present work was to investigate the validity of computing the instantaneous phase of a broad band signal.

Most classically trained physicists intuitively regard phase as a quantity that is meaningful only for single-frequency sinusoids. This understanding probably arises because the concept of phase is universally taught in signal processing courses using phasors. A phasor is a rotating vector that represents a wave. At any given time point in a phasor’s rotation in a Cartesian coordinate system, the y -coordinate of the phasor’s tip gives the amplitude of the wave and the angle between the phasor and the x -axis gives the instantaneous phase, or phase angle, of the wave. From this perspective, specifying “the instantaneous phase” of a broadband signal containing many harmonic components at different frequencies is not intuitively sensible, since many different phasors are involved, each rotating at a different angular frequency. Hence the conviction (e.g. [Pikovsky et al., 2001](#)) that in order meaningfully to measure instantaneous phase, one must first filter one’s data into a narrow pass band.

However, against this intuitive reaction must be set the findings of the present study.

[Fig. 3](#) serves as an intuition pump to illustrate not only the use of the SAPD metric in general, but also the meaning of broad band phase synchrony. When the time series of two channels are per-

fectly in phase, the SAPD is low. During time periods when the two channels are not in phase, the SAPD is high. Thus, the intuitive meaning of broad band phase is that two broad band signals are in phase synchrony when they wax and wane in identical fashion.

[Appendix A](#) then derives a mathematical meaning for the concept of broad band phase. For a sinusoid of a single frequency, analytic phase as measured using the Hilbert transform very closely approximates instantaneous phase as calculated from the phasor. For broad band signals, [Appendix A](#) shows that analytic phase is simply the angle of a resultant phasor constructed from the multiple individual phasors associated with each of the individual frequency components of the signal.

Construction of a resultant phasor for a composite signal consisting of multiple individual signals of the same frequency has been an accepted procedure in ac circuit theory for well over a century ([Kennelly, 1893](#)). Essentially, all we are doing is extending that procedure to composite waves consisting of multiple individual signals of *different* frequencies. Clearly there is no computational objection to doing this – the issue is whether or not any physical meaning attaches to the results. [Boashash \(1992\)](#), for example, declares that deriving the instantaneous frequency of a multicomponent signal is nonsensical. The instantaneous frequency of a signal is the time-derivative of the instantaneous phase, so if it is true that instantaneous frequency has no physical meaning for broad band signals, does it not follow that instantaneous phase has no meaning for broad band signals either? We

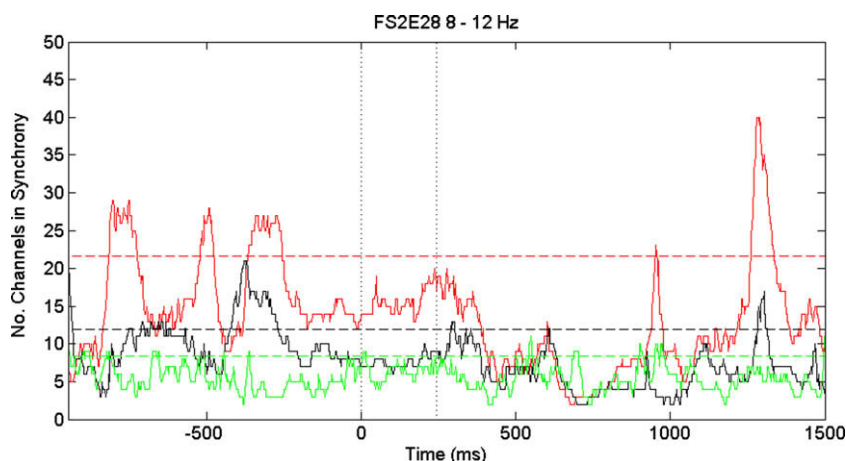


Fig. 9. Time series as for Fig. 4: 8–12 Hz.

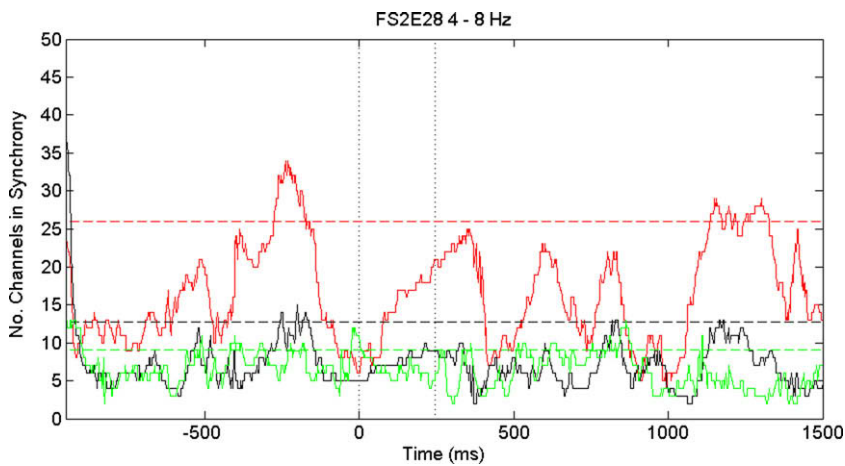


Fig. 10. Time series as for Fig. 4: 4–8 Hz.

argue that it does not follow. The opposition to use of instantaneous frequency for a multicomponent signal is that such a signal does not have a single frequency. But at any particular instant in time a multicomponent signal does have a single, well-defined

phase. Crudely put, instantaneous phase is a measure of whether the signal is near a peak, an axis-crossing, or a trough. Comparison of the instantaneous phases of two or more broad band signals is a perfectly legitimate way of determining whether the peaks, cross-

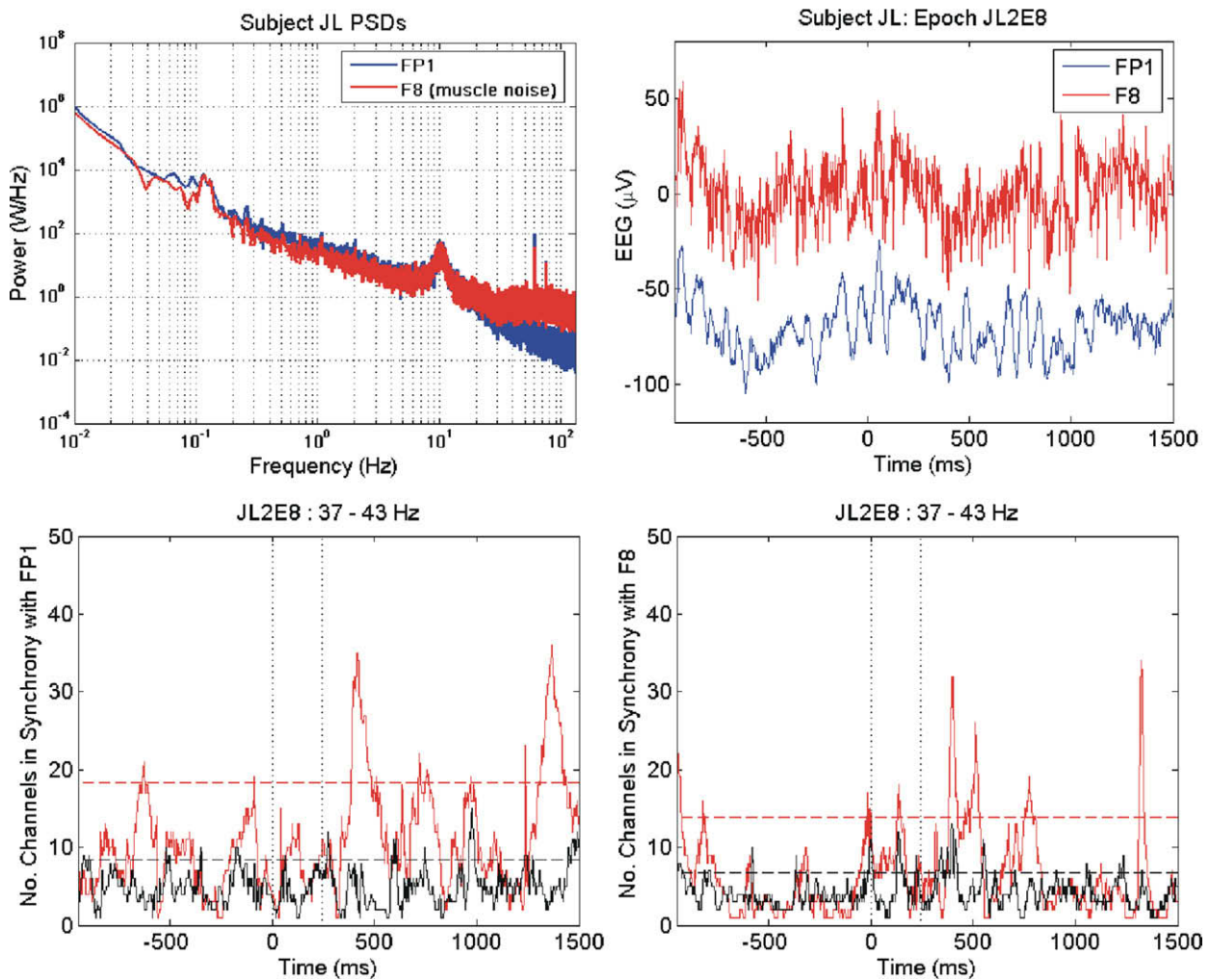


Fig. 11. Effect of muscle noise at the synchrony reference. Top left: power density spectra of noisy (red) and quiet (blue) channels. Top right: raw EEG from noisy (red) and quiet (blue) channels. Bottom left: time series for number of channels in synchrony with quiet channel (37–43 Hz). Bottom right: time series for number of channels in synchrony with noisy channel (37–43 Hz) for the same epoch as bottom left. (For interpretation of the references to color in this figure legend, the reader is referred to the web version of this paper.)

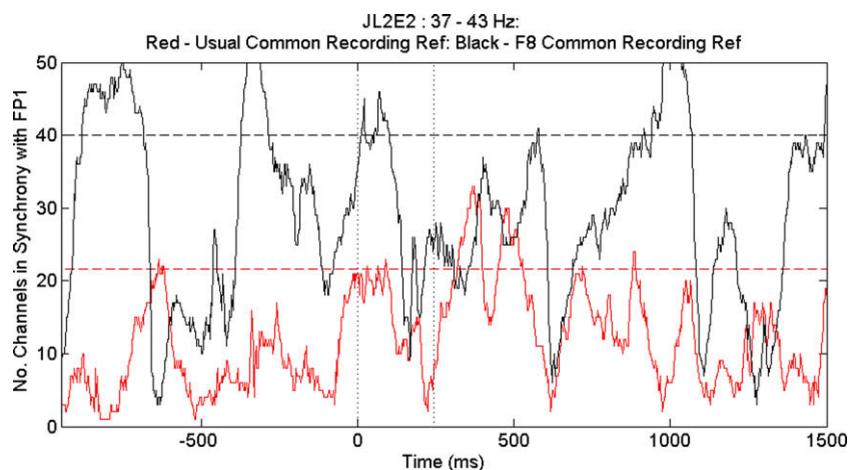


Fig. 12. Effect of muscle noise at common recording reference. Time series of number of channels in synchrony (37–43 Hz) for a different epoch of data from the same subject as Fig. 11: usual common recording reference (red); all data rereferenced to the muscle-noisy channel F8 (black). (For interpretation of the references to color in this figure legend, the reader is referred to the web version of this paper.)

ings, and troughs of those signals occur synchronously. We conclude that using the instantaneous phase of a broad-band (and thus potentially multicomponent) signal to measure synchrony between different signals is a well-founded project.

4.2. Potential artifacts

Two potential sources of artifactual synchrony were investigated.

4.2.1. Common reference artifact

A perennial problem with measuring synchrony in EEG data is that voltage has to be measured between two sites on the head. Any EEG measurement represents the voltage difference between a recording site, V_1 and a reference site, V_{ref} . As pointed out by [Fein et al. \(1988\)](#), any major reduction in power under electrode V_1 will cause the measurement $V_1 - V_{\text{ref}}$ to be dominated by activity under the reference electrode, V_{ref} . This has the potential to cause artifactual synchrony, due to the comparison of two measurements both of which are dominated V_{ref} .

One standard way of getting around this problem is to re-reference all data to an average reference. This is done by subtracting from each electrode the average of the voltages recorded at all electrodes on the head at that time point. Supposing for ease of explanation that there are only two electrodes on the head (although actually in our case there are 64), this works in the following way:

$$\begin{aligned} & (V_1 - V_{\text{ref}}) - (((V_1 - V_{\text{ref}}) + (V_2 - V_{\text{ref}}))/2) \\ &= (V_1 - V_{\text{ref}}) - (V_1 + V_2)/2 - (-2V_{\text{ref}}/2) \\ &= V_1 - V_{\text{ref}} - (V_1 + V_2)/2 + V_{\text{ref}} = V_1 - (V_1 + V_2)/2 \end{aligned}$$

Thus does simple algebra dictate that re-referencing to an average reference removes the reference electrode from the equation altogether. However, the problem with re-referencing to an average reference is that not only will it remove any artifactual synchrony resulting from dominance of the reference electrode – it will also remove much of any genuine widespread synchrony that might exist. The average that is being subtracted here essentially represents the activity that all electrodes have in common, which is exactly what we are trying to measure.

One way around this is to plot SAPD values for both average-referenced and common-referenced data on the same graph, as we have done in [Figs. 3–10](#). As shown above, any synchrony that re-

mains in average-referenced data cannot logically be due to the artifact postulated by [Fein et al. \(1988\)](#). Episodes of synchrony in average-referenced data are genuine. While it is theoretically possible that some episodes of common-referenced synchrony may be artifactual, there is no reason to suppose that episodes of genuine, average-referenced synchrony should occur at the same time as artifactual episodes of common-referenced synchrony. Yet our data show that smaller but still clearcut episodes of average-referenced synchrony do occur at the same time as many if not most episodes of common-referenced synchrony. We conclude that such episodes of synchrony are genuine, and that the actual number of channels in synchrony during them is more accurately represented by common-referenced than average-referenced data.

There are a few episodes of common-referenced synchrony in our data that are not paralleled by episodes of average-referenced synchrony. It is possible (though we think it unlikely) that these episodes may be artifacts of a sudden decrease of power in comparison with the reference under all of the recording electrodes involved in the episode, but none of the recording electrodes not involved in the episode.

4.2.2. Muscle noise artifact

A second potential source of artifact is muscle noise. It has long been known that gamma EEG can be significantly contaminated by muscle noise (e.g. [Freeman et al., 2003b](#)), and [Whitham et al. \(2007\)](#) have recently shown that in their subjects much of the EEG power above 20 Hz disappeared during experimental muscle paralysis.

There are two ways in which muscle noise might affect SAPD, depending on whether the muscle noise is evident at the synchrony reference channel or the recording reference channel.

(a) The predicted effect of muscle noise at the *synchrony* reference channel (i.e. the channel whose degree of synchrony with all other channels is being measured) is not immediately obvious. A priori there are three possibilities: muscle noise on the synchrony reference could artifactually (i) increase the incidence of widespread synchrony, (ii) decrease the incidence of widespread synchrony, or (iii) have no effect on the incidence of widespread synchrony. [Fig. 11](#) investigates which of these options applies in our data. The top left panel of [Fig. 11](#) superimposes the power spectrum of a non-noisy channel (represented in blue in both this panel and the top right panel) with a particularly noisy channel in the right temporal region (red in both panels). This subject was particularly prone to teeth-clenching, which suggested that the

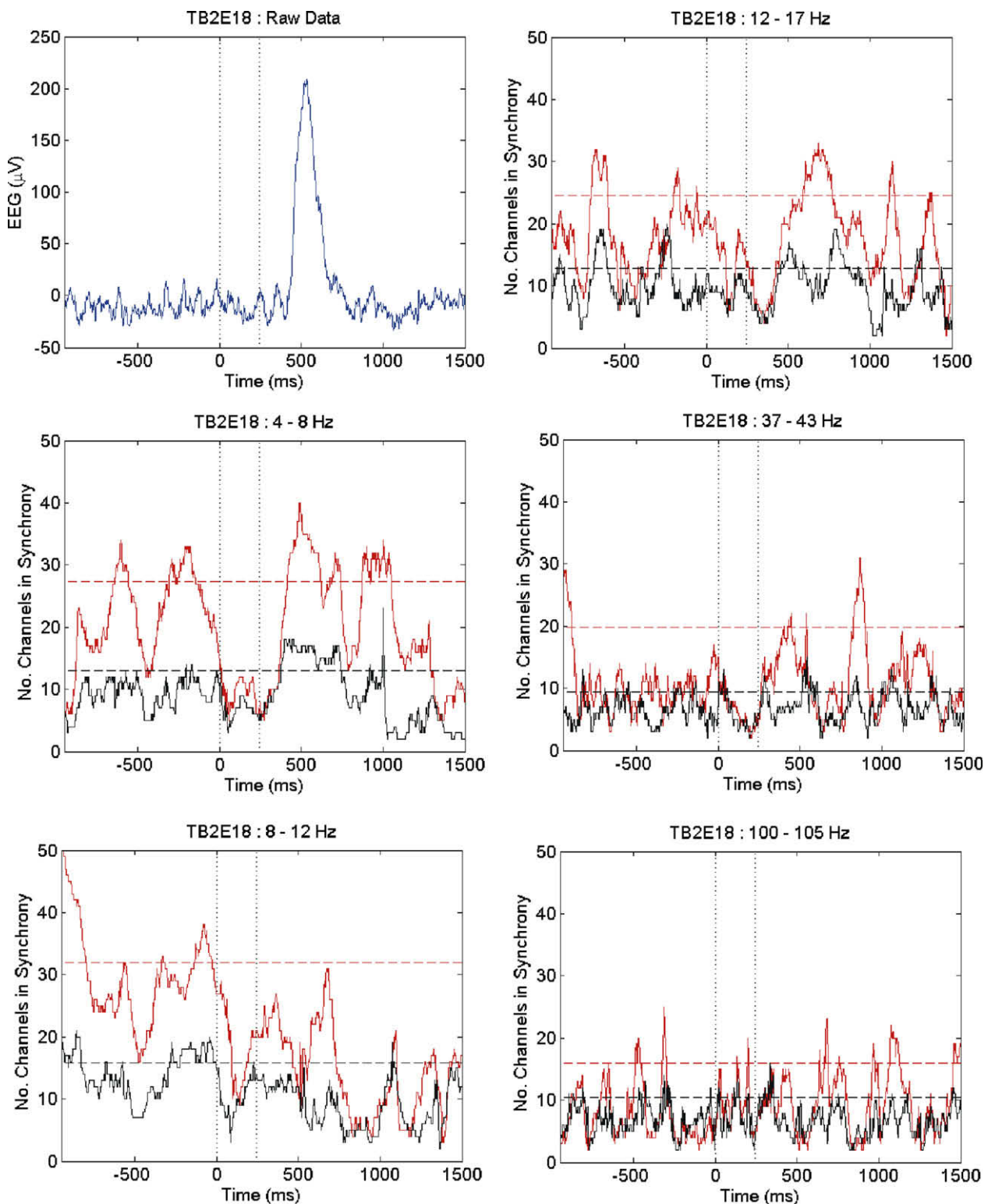


Fig. 13. Effect of a blink. Top left: raw data from channel FP1 showing one blink. Middle left: time series for number of channels in synchrony with FP1, same epoch as top left, 4–8 Hz. Bottom left: as for middle left but 8–12 Hz. Top right: as for middle left but 12–17 Hz. Middle right: as for middle left but 37–43 Hz. Bottom right: as for middle left but 100–105 Hz. Red and black lines in panels other than top left indicate number of channels in synchrony for common recording referenced data and average recording referenced data, respectively, as for Figs. 4–10. (For interpretation of the references to color in this figure legend, the reader is referred to the web version of this paper.)

consistent noise seen on F8 might be muscle noise. The top left panel shows that the power spectrum of F8 is virtually identical to the power spectrum of the other channel up to 20 Hz, where the spectrum of F8 flattens out to approximate white noise. Twenty hertz is exactly the frequency identified by Whitham et al.

(2007) as the point above which EMG contamination comes into play in scalp EEG and Freeman et al. (2003a) have shown that voluntarily produced scalp muscle noise has the flat spectrum of white noise, so the top left panel of Fig. 11 tends to confirm the origin of the noise on subject JL's channel F8 as muscle activity.

Accepting this interpretation, comparison of the bottom two panels of Fig. 11 shows that option (i) above does not obviously apply. The incidence of widespread synchrony is not increased when the synchrony reference is the muscle-noisy channel F8. The pattern of synchrony episodes is similar for both noisy and relatively quiet synchrony references, with the duration of the episodes being if anything reduced with the noisy synchrony reference. In the absence of a complex statistical treatment which does not seem justified in this circumstance, it is not clear whether option (ii) (muscle-related decrease in widespread synchrony) or option (iii) (no change) is closer to the truth. But what is clear from Fig. 11 is that continuous muscle noise on the synchrony reference does not cause continuous widespread synchrony. With a continuously muscle-noisy synchrony reference, widespread synchrony is still episodic. Furthermore, the episodes of widespread synchrony by and large occur at the same times as similar episodes measured with a less noisy synchrony reference (compare the bottom two panels of Fig. 11). This would perhaps be expected given the peak numbers of channels in synchrony. We therefore conclude that any effect of muscle noise at the synchrony reference is minor.

(b) The predicted effect of muscle noise at a common recording reference would be to increase power at the recording reference and thus exacerbate the artifact described in (1) above. Fig. 12 shows that rereferencing data to a particularly noisy recording reference (the same F8 investigated in Fig. 11) does indeed greatly increase the peak numbers of channels in synchrony. However, the widespread synchrony seen with this noisy common recording reference is still episodic rather than continuous. Furthermore, the episodes of synchrony have roughly the same durations and frequency as those seen with a quieter common recording reference. The top right panel of Fig. 11 shows that the muscle noise at the chosen recording reference is not itself obviously episodic, which again suggests that the episodes of widespread synchrony seen with the muscle-noisy recording reference are not simply due to episodic muscle noise, but have at least something to do with brain activity.

A third way in which muscle-related noise might affect or produce artefactual synchrony is via blinks. Blinks were rare in our data, because the subjects were instructed to avoid blinking until after feedback on the task had been given. All of the epochs analysed for the present report, including those shown in Supplementary Figs. S1–S12, were free of blinks in prefrontal channels. However, for completeness, Fig. 13 shows the relationship between one blink and the number of channels in synchrony for a standard series of passbands. The top left panel of Fig. 13 shows raw EEG recorded at the prefrontal channel FP1 for one blink-contaminated epoch (this epoch was not among those analysed in the rest of the paper). The large amplitude of the blink relative to the background noise clearly indicates the time at which the blink occurred. The other three panels of Fig. 13 show that for most passbands there is indeed, in this particular epoch, an episode of synchrony at approximately the time of the blink. However, this episode is unremarkable in comparison with the numerous other synchrony episodes that occur at times when there was clearly no blink. Fig. 13 thus demonstrates that (a) our initial visual screening process would have revealed any blinks in the epochs analysed in the rest of the paper and (b) our main result – that there are episodes of widespread synchrony at all passbands – cannot be dismissed as being merely an artifact due to blinks.

4.3. Comparison of our results with the literature

Our present finding of intermittent long-range synchrony at all passbands from theta to epsilon (aka high gamma) conflicts with the suggestion (Kopell et al., 2000; Von Stein and Sarnthein,

2000; Von Rullen and Koch, 2003) that long-range synchrony occurs only in low frequency bands (Arieli et al., 1995), while gamma oscillations are synchronous only in local networks or at most between a few cortical areas (Eckhorn, 1994; Steriade et al., 1996; Engel et al., 1991b; Roelfsema et al., 1997). In fact the suggestion that theta/alpha or theta/alpha/beta synchrony is global while gamma or beta/gamma-synchrony is local has already been negated by numerous reports of long-range gamma synchrony coinciding with various conscious experiences (Haig et al., 2000; Bhattacharya et al., 2001; Gruber et al., 2001; Lutz et al., 2002; Summerfield and Mangels, 2005). We confirm that long-range synchrony is widespread in theta, alpha, beta, gamma and epsilon bands – and in fact is sometimes more widespread in gamma and epsilon bands than at lower frequencies. We add the finding that long-range beta synchrony not only coincides with the perception of particular experimentally induced conscious experiences, but also occurs intermittently throughout the recorded dataset.

4.4. Possible mechanisms of generation of global synchrony

In principle, there are a number of means by which global inter-channel synchrony like that reported here might be established.

(1) First, the possibility must be considered that some of the synchrony we see could be an artifact of volume conduction. That all of it is due to volume conduction is extremely unlikely, as shown by the occasional presence of in-phase synchrony between our prefrontal reference channels and channels at the extreme rear of the head, with extensive areas of anti-phase synchrony or no synchrony at all in between.

(2) Second, the inverse problem is an ever-present barrier to confident interpretation of scalp-recorded EEG data. The natural assumption that activity recorded at EEG channel x reflects neural activity occurring under electrode x is dicey at best. It is possible that what we are seeing is nothing more than the signature of one or more strong dipoles in the middle of the brain. This might, for example, explain the fore-aft antisynchrony (i.e. out-of-phase synchrony) seen to varying degrees in the left hemispheres of subject FS (and also subjects ZY, KK and CJ, not shown) in the Supplementary Movies. However, it could not explain the lack of such fore-aft antisynchrony in the right hemispheres of these subjects, or in either hemisphere of the other two subjects. The possibility that central dipoles are the entire explanation of our results is also rendered unlikely by the findings of (a) strong in-phase (rather than out-of-phase) synchrony between prefrontal and some occipital channels and (b) distinctly non-dipolar overall structure of the observed areas of out-of-phase synchrony.

(3) A separate but related possibility is that proposed by Llinas and Ribary (Ribary et al., 1991; Joliot et al., 1994; Llinas et al., 1998). These authors propose that a thalamic pacemaker, driven by the intrinsic properties of the ionic conductances in various kinds of thalamic cell and modified by sensory input, may be responsible for the coherence of 40-Hz cortical rhythms they observe. This mechanism could certainly explain some of our findings.

(4) A fourth possibility is proposed by Wolf Singer's group. These workers suggest, on the basis of observed loss of interhemispheric synchrony after cutting the corpus callosum, that long-range synchrony is mediated by axonal conduction between the synchronous areas of cortex (Engel et al., 1991a,b, 2001). Simulations have found that zero-lag synchrony can be established by this means provided the axonal conduction time between the synchronous regions of cortex does not exceed one third of the cycle time of the oscillation (König and Schillen, 1991). Our finding that it takes of the order of 100 ms for episodes of global synchrony to become fully established suggests that chemical synapses are likely

to be the mechanism of establishment of widespread synchrony. It could be argued that this mechanism is too imprecise to allow long-term maintenance of widespread synchrony. Our finding that episodes of widespread synchrony are relatively brief again accords with the idea that normal synaptic transmission is the relevant mechanism.

(5) A fifth possibility is suggested by the hypothesis that the brain should be looked at in terms of a neural field theory, which sees cortical signals as continuously distributed in the neuropil (Gerard, 1936; Freeman, 2005). While a field theoretic viewpoint in general may be useful from the point of view of thinking about the topology brain function, it is hard to envisage a physical mechanism by which one part of a mathematically described field could communicate with another part 300 mm away unless one equates the hypothetical field with the electromagnetic field. Doing this immediately raises the spectre of Köhler's electric field theory of brain function (Köhler, 1940) which is widely supposed to have been disproved half a century ago by Lashley and Semmes (1951) and Sperry et al. (1955). But the theory tested by Lashley and Sperry was quite different from the present suggestion. In Köhler's day, so little was known about cellular neurophysiology that it was reasonable for him to propose that the visual system might function by means of extracellular current flow from site to site in the cortex, with a figure being represented by a dense continuous current flow and contours by gradients in the intensity of flow. Lashley and Sperry did indeed claim to have disproved this hypothesis: Lashley by inserting gold pins into or laying gold strips over the cortex of monkeys with the aim of short-circuiting the hypothesized figure currents and showing that the monkeys could still perform a previously learned visual task, and Sperry by doing a similar experiment with tantalum pins in cats. But we are not suggesting that the visual system functions by means of transcortical extracellular currents – only that an ongoing neuronally generated electric field might act as a synchronizing influence on the firing of neurons at widely different cortical sites, on the principle of circular causation (Freeman, 2006). From the vantage point of the early 21st century, it is difficult to see how the insertion of a few metal pins into the cortex could prevent such a synchronizing influence. So a brain-wide extracellular electromagnetic field might exert some synchronizing effect. However, this effect should be more or less instantaneous, which does not accord with our finding that it takes ~100 ms for episodes of global synchrony to become established.

(6) A variant of the extracellular electric field idea is that a series of interneuronal gap junctions might perform a synchronizing function by means of electrical transmission, recalling John's speculative "hyperneuron" (John, 2006). Initially this suggestion would seem to be rendered unlikely by our present finding that it takes about 100 ms for an episode of synchrony to become established. It is widely believed that the synaptic delay for a chemical synapse is about 2 ms, while the synaptic delay for an electrical synapse is about 0.2 ms. However, this difference may be minimised at mammalian body temperatures, where chemical synaptic delays can be as short as 150 μ s (Sabatini and Regehr, 1996). Electrical transmission through gap junctions does seem to be involved in synchronization of activity between neurons up to about 200 μ m apart (Connors and Long, 2004), but it remains to be seen whether gap junctions are involved in longer-range synchronization of neural activity. That they may not be vital is suggested by the finding that mice with targeted deletion of any of a number of connexins (the protein substrates of gap junctions) still show relatively normal brain function (Bennett and Zukin, 2004).

(7) Quantum non-locality has been suggested as a mechanism by which global synchrony might be established. Our finding that the establishment of individual episodes of widespread synchrony is far from instantaneous probably rules out this idea.

(8) A final possibility to be considered is that the brain as a system might function in a state of self-organized criticality (Schroeder, 1991; Bak, 1997; Jensen, 1998; Linkenkaer-Hansen et al., 2001; Freeman, 2005). The time course of synchrony establishment in such a system remains to be established.

It seems to us quite likely that some time-varying combination of several of these mechanisms may be involved in generation of the synchrony we observe, although chemical synaptic transmission is likely to be the main determinant.

Acknowledgments

Thanks are due to Professor Robert T. Knight for access to hardware, Clay Clayworth for help setting it up and Christina Karns for assistance with stimulus software. Thanks also to Professor Stanley Klein for partial salary support to S.P. during the period of data collection. Alexander V.H. McPhail contributed useful discussions on the concept of broad band phase and much appreciated help with the writing of analysis software.

Appendix A. The meaning of instantaneous phase as applied to broad band signals

The hypothesis investigated in this appendix is that for a broad band signal, instantaneous phase as derived from the Hilbert transform = instantaneous phase as derived by taking, at each time point, the angle of the resultant of the phasors of all the component waves making up the broad-band signal.

In real EEG data, the characteristics of the component waves making up any given broad-band signal are not known, so the second part of the hypothesized identity cannot be calculated. We therefore start with three artificially generated sinusoids, which can be described in polar coordinates as:

$$\begin{aligned} S_1 &= e^{i(\omega_1 t + \phi_1)}, \\ S_2 &= e^{i(\omega_2 t + \phi_2)}, \\ S_3 &= e^{i(\omega_3 t + \phi_3)}. \end{aligned}$$

The three sinusoids are combined to form a broad-band signal

$$S = S_1 + S_2 + S_3.$$

To this broad-band signal we apply the Matlab command 'angle', which extracts the resultant of the instantaneous phase angles ϕ_1 , ϕ_2 and ϕ_3 at each time point.

Because knowledge of the individual components making up a broad band signal is not needed in order to calculate the instantaneous phase of that signal using the Hilbert transform, it is possible to find this version of instantaneous phase for real EEG data. However, for the purposes of this hypothesis test, we now calculate the Hilbert transform side of the hypothesized identity using the same three artificial sinusoids. This time they may be conveniently expressed in Cartesian coordinates:

$$\begin{aligned} h_1 &= \cos(\omega_1 t + \phi), \\ h_2 &= \cos(\omega_2 t + \phi), \\ h_3 &= \cos(\omega_3 t + \phi). \end{aligned}$$

The three sinusoids are again combined, to give the same broad-band signal, now called

$$h = h_1 + h_2 + h_3.$$

Application of the Matlab command 'hilbert' to h gives the analytic signal

$$h_A = h + j\hat{h} \quad \text{where } \hat{h} = \text{the Hilbert transform of } h.$$

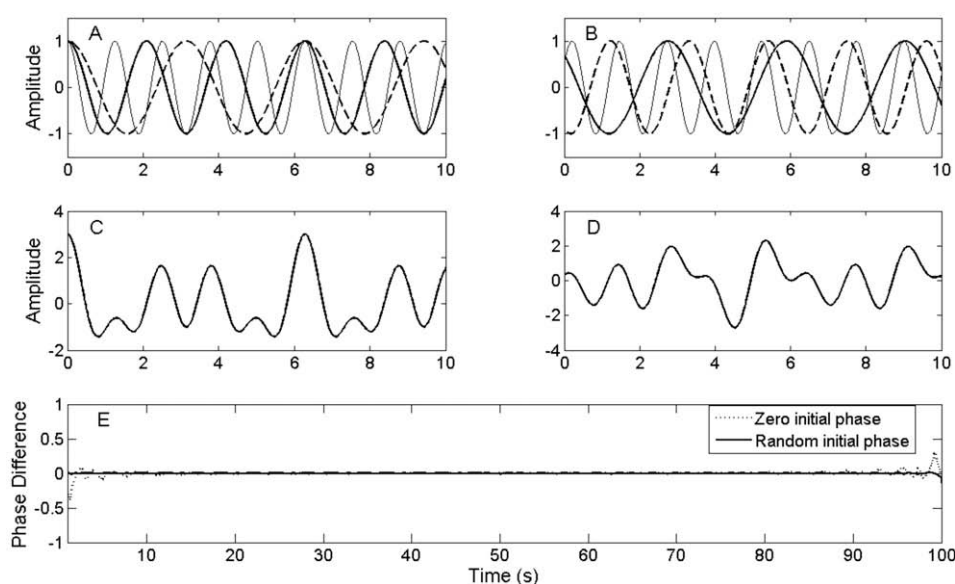


Fig. A1. Comparison of analytic phase and phasor-derived instantaneous phase for artificial composite signals. (A) Three sine waves. (B) Three waves with same frequencies as those in A but starting at random points in their cycles. (C) Composite wave generated by adding the three waves in A. (D) Composite wave generated by adding the three waves in B. (E) Differences between analytic phase and phasor-derived instantaneous phase for the two waves in C and D.

Application of 'angle' to h_A then gives a second version of instantaneous phase.

Fig. A1 compares instantaneous phase computed in each of these two ways for a broad band signal generated by adding three artificial sine waves of different frequencies. Using the artificial signals in Fig. A1C and D (which are, respectively, composed of the three cosine waves in Fig. A1A and B), Fig. A1E shows that the relationship between instantaneous phase as computed via the Hilbert transform and instantaneous phase as derived from the phasors of the individual cosine waves depends on whether the three component waves begin at the same point in their cycles, or at randomly distributed points. In both cases the two versions of instantaneous phase are virtually identical in the middle of the data segment. The only difference between the two cases is that the edge effects are more serious in the case where the component waves all start at the same point in their cycle. Since this condition would virtually never hold for the component waves making up a real EEG signal, we conclude that taking the instantaneous phase of a broad-band signal using the Hilbert transform is equivalent to taking the resultant of the phases of the all the hypothetical single-frequency components making up the broad-band signal.

Appendix B. Supplementary data

Supplementary data associated with this article can be found, in the online version, at doi:10.1016/j.clinph.2008.12.044.

References

- Arieli A, Shoham D, Hildesheim R, Grinvald A. Coherent spatiotemporal patterns of ongoing activity revealed by real-time optical imaging coupled with single-unit recording in the cat visual cortex. *J Neurophysiol* 1995;73:2072–93.
- Bak P. *How nature works? The science of self-organized criticality*. Oxford: Oxford University Press; 1997.
- Bennett MVL, Zuckin RS. Electrical coupling and neuronal synchronization in the mammalian brain. *Neuron* 2004;41:495–511.
- Bhattacharya J, Petsche H. Phase synchrony analysis of EEG during music perception reveals changes in functional connectivity due to musical expertise. *Signal Process* 2005;85:2161–77.
- Bhattacharya J, Petsche H, Pereda E. Long-range synchrony in the gamma band: role in music perception. *J Neurosci* 2001;21:6329–37.
- Boashash B. Estimating and interpreting the instantaneous frequency of a signal. Part 1. Fundamentals. *Proc IEEE* 1992;80:520–37.
- Bracewell RN. *The Fourier transform and its applications*. New York: McGraw-Hill; 1965.
- Connors BW, Long MA. Electrical synapses in the mammalian brain. *Ann Rev Neurosci* 2004;27.
- Eckhorn R. Oscillatory and non-oscillatory synchronizations in the visual cortex and their possible roles in associations of visual features. *Prog Brain Res* 1994;102:405–26.
- Engel AK, König P, Kreiter AK, Singer W. Interhemispheric synchronization of oscillatory neuronal responses in cat visual cortex. *Science* 1991a;252:1177–9.
- Engel AK, Kreiter AK, König P, Singer W. Synchronization of oscillatory neuronal responses between striate and extrastriate visual cortical areas of the cat. *Proc Natl Acad Sci USA* 1991b;88:6048–52.
- Engel AK, Fries P, Singer W. Dynamic predictions: oscillations and synchrony in top-down processing. *Nat Rev* 2001;2:704–16.
- Fein G, Raz J, Brown FF, Merrin EL. Common reference coherence data are confounded by power and phase effects. *Electroenceph Clin Neurophys* 1988;69:581–4.
- Freeman WJ. Origin, structure and role of background EEG activity. Part 1. Analytic amplitude. *Clin Neurophysiol* 2004a;115:2077–88.
- Freeman WJ. Origin, structure, and role of background EEG activity. Part 2. Analytic phase. *Clin Neurophysiol* 2004b;115:2089–107.
- Freeman WJ. A field-theoretic approach to understanding scale-free neocortical dynamics. *Biol Cybernet* 2005;92(6):350–9.
- Freeman WJ. Consciousness intentionality and causality. In: Pockett S, Banks WP, Gallagher S, editors. *Does consciousness cause behavior?* Boston (MA): MIT Press; 2006. p. 73–105.
- Freeman WJ. Definitions of state variables and state space for brain-computer interface. Part 1. Multiple hierarchical levels of brain function. *Cog Neurodyn* 2007;1:3–14.
- Freeman WJ, Rogers LJ. Fine temporal resolution of analytic phase reveals episodic synchronization by state transitions in gamma EEGs. *J Neurophys* 2002;87:937–45.
- Freeman WJ, Burke BC, Holmes MD. Aperiodic phase re-setting in scalp EEG of beta-gamma oscillations by state transitions at alpha-theta rates. *Hum Brain Map* 2003a;19:248–72.
- Freeman WJ, Holmes MD, Burke BC, Vanhatalo S. Spatial spectra of scalp EEG and EMG from awake humans. *Clin Neurophysiol* 2003b;114:1053–68.
- Gerard RW. Factors controlling brain potentials. *Cold Spring Harb Symp Quant Biol* 1936;4:292–304.
- Gruber T, Keil A, Müller MM. Modulation of induced gamma band response and phase synchrony in a paired associate learning task in the human EEG. *Neurosci Lett* 2001;316:29–32.
- Haig AR, Gordon E, Wright JJ, Meares RA, Bahramali H. Synchronous cortical gamma-band activity in task-relevant cognition. *Neuroreport* 2000;11(4):669–75.
- Jensen HJ. *Self-organized criticality: emergent complex behavior in physical and biological systems*. New York: Cambridge University Press; 1998.
- John ER. The sometimes pernicious role of theory in science. *Int J Psychophysiol* 2006;62:377–83.
- Joliot M, Ribary U, Llinas R. Human oscillatory brain activity near 40 Hz coexists with cognitive temporal binding. *Proc Natl Acad Sci USA* 1994;91:11748–51.

- Kennelly AE. Impedance. *Trans AIEE* 1893;10:175–232.
- Köhler W. Dynamics in psychology. New York: Grove Press; 1940.
- König P, Schillen TB. Stimulus-dependent assembly formation of oscillatory responses: I. Synchronization. *Neural Comp* 1991;3:155–66.
- Kopell N, Ermentrout GB, Whittington MA, Traub RD. Gamma and beta rhythms have different synchronization properties. *Proc Nat Acad Sci USA* 2000;97:1867–72.
- Lamme VAF, Spekrijse H. Neuronal synchrony does not represent texture segregation. *Nature* 1998;396:362–6.
- Lashley KS, Semmes KLC. An examination of the electric field theory of cerebral integration. *Psych Rev* 1951;58:123–36.
- Linkenkaer-Hansen K, Nikouline VV, Palva JM, Ilmoniemi RJ. Long-range temporal correlations and scaling behavior in human brain oscillations. *J Neurosci* 2001;21:1370–7.
- Llinas R, Ribary U, Contreras D, Pedroarena C. The neuronal basis for consciousness. *Philos Trans Roy Soc B* 1998;353:1841–9.
- Lutz A, Lachaux J-P, Martinerie J, Varela FJ. Guiding the study of brain dynamics by using first-person data: synchrony patterns correlate with ongoing conscious states during a simple visual task. *Proc Nat Acad Sci USA* 2002;99:1586–91.
- Pikovsky A, Rosenblum M, Kurths J. Synchronization: a universal concept in nonlinear sciences. Cambridge: Cambridge University Press; 2001.
- Ribary U, Ioannides AA, Singh KD, Hasson R, Bolton JPR, Lado F, et al. Magnetic field tomography of coherent thalamocortical 40-Hz oscillations in humans. *Proc Natl Acad Sci USA* 1991;88:11037–41.
- Rodriguez E, George N, Lachaux J-P, Martinerie J, Renault B, Varela FJ. Perception's shadow: long-distance synchronization of human brain activity. *Nature* 1999;379:430–3.
- Roelfsema PR, Engel A, König P, Singer W. Visuomotor integration is associated with zero time-lag synchronization among cortical areas. *Nature* 1997;385:157–61.
- Sabatini BL, Regehr WG. Timing of neurotransmission at fast synapses in the mammalian brain. *Nature* 1996;384:170–2.
- Schroeder M. Fractals, chaos, power laws. Minutes from an infinite paradise. New York: W.H. Freeman; 1991.
- Shadlen MN, Movshen JA. Synchrony unbound: a critical evaluation of the temporal binding hypothesis. *Neuron* 1999;24:67–77.
- Sperry RW, Miner N, Myers RE. Visual pattern perception following subpial slicing and tantalum wire implantations in the visual cortex. *J Comp Physiol Psychol* 1955;47:50–8.
- Steriade M, Amzica F, Contreras D. Synchronization of fast (30–40 Hz) spontaneous cortical rhythms during brain activation. *J Neurosci* 1996;16:392–417.
- Summerfield C, Mangels JA. Functional coupling between frontal and parietal lobes during recognition memory. *Neuroreport* 2005;16(2):117–22.
- Trujillo LT, Peterson MA, Kaszniak AW, Allen JJB. EEG phase synchrony differences across visual perception conditions may depend on recording and analysis methods. *Clin Neurophysiol* 2005;116:172–89.
- Von Rullen R, Koch C. Is perception discrete or continuous? *Trends Cog Sci* 2003;7:207–13.
- Von Stein A, Sarnthein J. Different frequencies for different scales of cortical integration: from local gamma to long range alpha theta synchronization. *Int J Psychophysiol* 2000;38:301–13.
- Whitham EM, Pope KJ, Fitzgibbon SP, Lewis T, Clark CR, Loveless S, et al. Scalp electrical recording during paralysis: quantitative evidence that EEG frequencies above 20 Hz are contaminated by EMG. *Clin Neurophysiol* 2007;118:1877–88.